Kinetic-energy release in CO dissociation caused by fast F^{4+} impact

I. Ben-Itzhak, S. G. Ginther, Vidhya Krishnamurthi, and K. D. Carnes
James R. Macdonald Laboratory, Department of Physics, Kansas State University, Manhattan, Kansas 66506
(Received 14 March 1994)

The dissociation of CO caused by 1-MeV/amu F^{4+} impact has been studied using the coincidence time-of-flight technique. The kinetic energy released during the dissociation of CO^{q+} into ion pairs C^{q_1+} and O^{q_2+} was determined from the measured difference in the times of flight of the two charged fragments. The kinetic-energy distributions of CO^{2+} dissociating into C^+ and O^+ as a result of different impinging projectiles have been compared. These distributions shift towards higher kinetic-energy release values with increasing strength of interaction. A single Gaussian kinetic-energy distribution is in good agreement with the highly charged CO dissociation, while for doubly and triply charged CO, additional Gaussians are needed. While the Coulomb-explosion model approximately predicts the most likely value of a measured distribution, the widths of all distributions are grossly underestimated by the model. The measured widths of the distributions can be explained only by invoking the existence of potential-energy curves of the multiply charged ions that have steeper and shallower slopes as compared to the Coulombic curve. The reflection method was used to calculate the kinetic-energy release for $F^{4+}+CO \rightarrow CO^{2+*}$ transitions to all known CO^{2+} states. The final kinetic-energy distribution was then fitted to the data in order to evaluate the weights of the different transitions. The calculated fit is in fair agreement with the measured one, although the high-energy tail of the measured distribution could not be accounted for, indicating that contributions from highly excited dissociating states or from curve crossings need to be included.

PACS number(s): 34.50.−s, 39.10.+j, 34.90.+q

I. INTRODUCTION

The dissociation process of singly and doubly charged molecular ions has been investigated extensively in the past using many different methods to remove the electrons from the molecule. Similar studies of the dissociation of multiply charged molecular ions have become a subject of increasing interest since it became possible to rapidly strip many electrons. Highly charged molecular ions can now be produced with negligible momentum transfer to the nuclei, thus making it possible to study the rearrangement of the electron "cloud" on the positive centers and the dissociation process itself. These highly charged molecular ions are produced by intense picosecond laser fields [1–4] or by fast highly charged ion impact from heavy-ion accelerators [5–9] and ion sources [10]. Another possible method used for fast multiple electron removal from molecules is by producing an inner-shell vacancy using synchrotron radiation [11–13]. Many electrons can be ejected if the vacancy is filled by an Auger process. The latter method is focused on the effect of inner-shell vacancies and their decay mechanisms while the first two methods are focused on the dissociation process caused by the removal of valence electrons.

We have used a 1-MeV/amu F^{4+} beam impinging on CO for which multiple ionization is the main rapid electron removal mechanism [14]. It has been shown for similar collisions on Ne targets that the recoil ion kinetic energy is very small because most of these collisions happen at relatively large impact parameters [15]. Thus the kinetic energy released (KER) in the dissociation can be evaluated by measuring the velocities of its fragments after the collision. The CO molecule was chosen as an example of a simple many-electron diatomic molecule bound by the L-shell electrons of both atoms. The fact that CO is a heteronuclear molecule makes it easier to distinguish the different charge states of the fragments in our time-of-flight spectrometer. Recently, studies of the kinetic energy released in CO dissociation following 2.4-MeV/amu Ar^{14+} impact have been reported by Sampoll *et al.* [16] and for 5.1-MeV/amu F^{8+} impact by Mathur *et al.* [17]. The kinetic energies released in CO dissociation following these collisions are somewhat different, but the reason for the differences is not yet well understood.

The kinetic energy released during the dissociation of a diatomic molecular ion into ion pairs can be evaluated using the Coulomb-explosion model. This model is expected to be valid if the two ions can be approximately treated as point charges moving away from each other because of the mutual Coulombic repulsion between them. This is equivalent to saying that the repulsive potential-energy curves are Coulombic, i.e., $V(R)=q_1q_2/R$. This model is expected to be valid for highly stripped CO and to break down for low charge states. The fact that for most highly charged molecular ions the potential curves have not been calculated makes the Coulomb-explosion model a very useful tool for calculating kinetic-energy releases in the dissociation of diatomic molecular ions. In this paper we probe the validity of this simple model and its limitations. The coincidence time-of-flight technique and the experimental apparatus

used for these studies have been described in detail elsewhere [9]. The experimental method used to measure and evaluate the kinetic-energy distributions of the different dissociation channels is discussed briefly in Sec. II. The role of non-Coulombic potential-energy curves in the dissociation of CO^{Q+} ($Q \geq 2$) into ion pairs and the validity of the Coulomb-explosion model are discussed in Sec. III. Our results are also compared in the same section to the kinetic-energy release in CO dissociation caused by other projectiles. Furthermore, we have tried to probe the existence of a propensity rule in the population of the dissociating CO^{2+} states of different symmetries. No such rule was found. We have seen indications, however, that there exists a window of transition energies within which the transition from CO to CO^{2+} is an efficient process.

II. EXPERIMENTAL METHOD AND DATA ANALYSIS

A detailed description of our experimental setup and the coincidence time-of-flight method used for this study can be found in previous publications [9,14]. Briefly, a bunched beam of F^{4+} was accelerated in the J. R. Macdonald Tandem Van de Graaff accelerator to an energy of 19 MeV and then selected by a 90° analyzing magnet. The collimated beam was then made to interact with CO under single-collision conditions. Ions produced in the cell's collision region were extracted and accelerated by uniform electric fields and allowed to drift into a large chevron microchannel plate detector. The kinetic energy released during the dissociation of the molecular ion was determined from the difference in the times of arrival of the different fragments ($t_{21}=t_2-t_1$, where t_1 and t_2 are the times of flight of the first and second fragments, respectively). The minimum separation time needed by the electronics is 11 nsec. Thus only time differences larger than 11 nsec can be measured. This limits the study of a few dissociation channels of CO, but causes no problem for most of the channels.

Typical time-difference spectra for the dissociation of CO^{3+} into $C^{2+}+O^{+}$ measured with strong and weak extraction fields are presented in Fig. 1. The distribution of time differences for a given dissociation channel is a result of the velocity distribution of the dissociating ions in the direction of the detector. Thus the time-difference spectrum contains information about both the kinetic-energy released and the angular distribution of the internuclear axis relative to the beam direction (see Fig. 2). If the fragment that hits the detector first is initially heading away from the detector, the time difference will be reduced; if it is initially heading toward the detector, it will increase. Molecules dissociating parallel to the detector plane will have a time difference that is independent of the kinetic energy released. For an isotropic dissociation, one expects a flat top time-difference peak if angular discrimination is negligible [9]. It can be seen from Fig. 1(a) that the $C^{2+}+O^{+}$ dissociation measured with a strong extraction field, where angular discrimination is expected to be negligible, has a relatively flat top time-difference peak. Deviations from isotropy in the multiple ionization of CO by F^{4+} are thus very small, if any, and

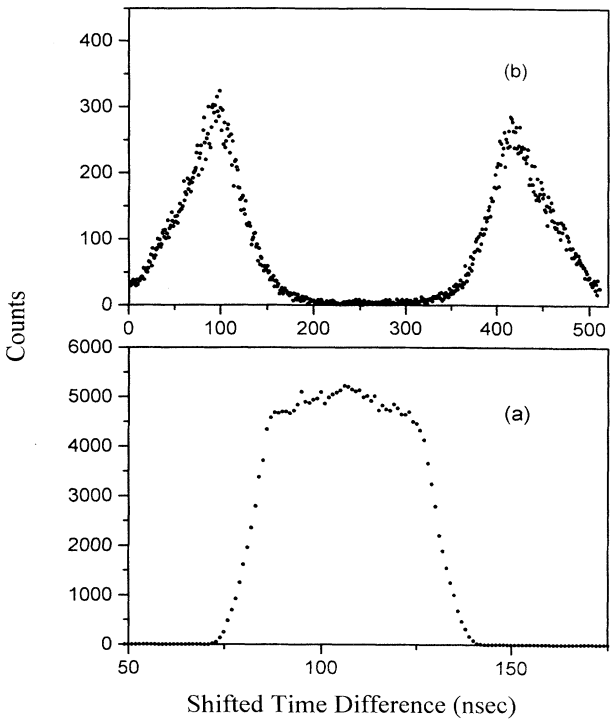

FIG. 1. Time-difference spectrum of $CO^{3+}\rightarrow C^{2+}+O^{+}$ dissociation caused by 1-MeV/amu F^{4+} impact. Measured with an extraction field of (a) 1250 V/cm and (b) 156 V/cm.

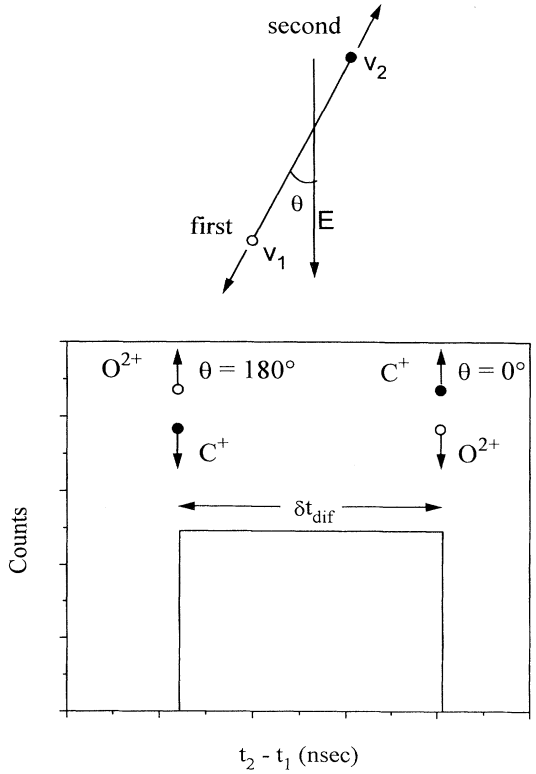

FIG. 2. Schematic view of the molecular alignment relative to the extraction field and the resulting time-of-flight differences, assuming no angular discrimination.

we have assumed isotropy for the data analysis in this study. Anisotropies in fast ion-molecule collisions are of increasing interest [18–20] and some angular dependences have been seen for electron-capture processes [19]. Multiple ionization, however, has been found to be mostly isotropic [20]. Multiple ionization is the main mechanism of electron removal in the $F^{4+}+CO$ collisions under study [14]; thus the dissociation is expected to be isotropic.

We have used two methods to evaluate the distribution of kinetic energy carried by the fragments from the time-difference spectrum of each breakup channel. The first method involves a measurement using a strong extraction field, thus minimizing angular discrimination and improving the collection efficiency. In the second method a weak extraction field was used, thus expanding the time-difference spectrum (as can be seen from Fig. 1) and improving the resolution of the kinetic-energy release. The "penalties" for the improved energy resolution, however, are strong angular discrimination, which complicates the data analysis, and a significant reduction in detection efficiency, especially for the breakup of highly charged CO. Both methods are described in some detail below. The strong-field method was used to determine the detailed kinetic-energy distribution of the main ion-pair dissociation channels, while the weak-field method was used to evaluate the most likely kinetic-energy release and the width of its distribution.

The strong-field method for determining the kinetic-energy distribution of the dissociation into ion pairs from the time-difference spectrum, where angular discrimination is negligible, has been discussed in detail by Schäfer *et al.* [21] and Ben-Itzhak, Ginther, and Carnes [22]. This method is based on the fact that a narrow range of energies dE_k around the kinetic-energy release E_k will produce a flat top distribution between the minimum and maximum time differences associated with the two molecular orientations along the extraction field, as shown schematically in Fig. 2. The width of such a contribution thus depends on the kinetic energy released in the dissociation while the height depends on the probability for this kinetic energy $P(E_k)$ (the second statement is correct only when angular discrimination is negligible). This relationship [Eq. (3) in Ref. [22]] can be written as

$$P(E_k)=[t_{21}(E_k,0°)-t_{21}(E_k,180°)]\frac{dt_{21}}{dE_k}\frac{dY}{dt_{21}}\ , \tag{1}$$

where $t_{21}(E_k,0°)$ and $t_{21}(E_k,180°)$ are the maximum (i.e., $\theta=0°$) and minimum (i.e., $\theta=180°$) time differences, respectively (θ is the angle between the internuclear axis and the extraction field, shown in Fig. 2). The time difference for $\theta=0°$ is given approximately by

$$t_{21}(E_k,0°)\simeq\frac{2}{\mathcal{E}_2}\left[\frac{1}{q_1}+\frac{1}{q_2}\right]\sqrt{2\mu E_k} \tag{2}$$

(with a similar expression for 180°), where $\mathcal{E}_2$ is the extraction field and μ is the reduced mass of the molecule. The exact time-difference formula for our time-of-flight spectrometer was used in the data analysis, but is too long to include here in detail. The time differences to be used in Eq. (1) are calculated for all possible kinetic-energy release values. dY/dt_{21} is the numerical time derivative of the large time-difference side of the spectrum, and dt_{21}/dE_k is evaluated at $\theta=0°$. The energy distributions can also be evaluated from the small time-difference side of the spectrum (see Ref. [22] for a detailed explanation).

The weak-field method can give a better energy resolution since the time-difference spectrum is significantly wider. (See, for example, Fig. 1.) But spectra measured with a relatively weak extraction field, such as the one shown in Fig. 1(b), will typically have a dip in the center because of large angular discrimination effects. (Molecules that dissociate perpendicular to the extraction field are not likely to be detected, while all the molecules oriented parallel to the field will reach the detector.) Because of this large angular discrimination it is hard to use the method discussed above to evaluate the kinetic-energy distribution from such measurements. One method commonly used in photoion photoion coincidence studies [11–13] is to start with a trial kinetic-energy release distribution $P(E_k)$ and then simulate the resulting time-difference spectrum for an isotropic distribution. This simulated spectrum is then compared with the measured one, the initial $P(E_k)$ is adjusted, and the process is repeated until the simulated time-difference spectrum is in reasonable agreement with the measured one. This method can be easily used for our spectrometer because the time-difference spectrum resulting from each kinetic-energy release E_k can be calculated analytically [9]. But, the trial and error nature of this method makes the process time consuming. Recently, Sampoll *et al.* [16] have used an iterative method suggested by Scofield in order to simplify the somewhat tedious search for the correct $P(E_k)$ after they have calculated the response function of their time-of-flight spectrometer using Monte Carlo simulations. As we were interested mainly in the general trends, we simplified the fitting procedure, for the measurements performed with a weak extraction field, by assuming a Gaussian distribution for the kinetic-energy release and then calculating the expected time difference for this distribution. The peak position and the full width at half maximum (FWHM) of these Gaussian distributions were evaluated by fitting the simulated time-difference spectrum to the measured one [23]. These values are presented in Table I. It will be shown later

TABLE I. Peak value of the kinetic-energy distribution (eV) (upper line) and FWHMs (lower line) of the fragmentation channels $C^{i+}+O^{j+}$ ($i,j=1$–4, excluding $i=j=4$).

	O^+	O^{2+}	O^{3+}	O^{4+}
C^+	10.5±1.5	35±3	60±10	70±5
	7±2	18±4	30±10	40±15
C^{2+}	26±2	56±4	95±2	105±15
	13±2	26±6	40±5	60±20
C^{3+}	50±5	78±7	105±10	150±20
	40±10	40±10	50±10	55±15
C^{4+}	55±5	80±10	105±15	
	30±10	50±10	50±15	

that such distributions reproduce the time-difference spectra nicely, except for a few dissociation channels in which only a few electrons were removed from the target molecule.

III. RESULTS AND DISCUSSION

It was shown in an earlier publication [14] that most transient multiply charged CO molecular ions produced in these collisions dissociate rapidly into ion pairs as expressed by

$$F^{4+}+CO\rightarrow CO^{Q+*}\rightarrow C^{q_1+}+O^{q_2+} . \quad (3)$$

The two charged fragments move away from each other because of the mutual Coulomb repulsion between them. If the electrons rearrange fast enough relative to the nuclear motion and the electron clouds around each center are tight in comparison with the internuclear separation ($R_0\sim 2.14$ a.u. for CO), one expects that the simple Coulomb-explosion model will be valid. In this model the two ions are treated as point charges whose initial energy is given by the Coulomb energy at the equilibrium internuclear distance R_0. This potential energy is converted into the kinetic energy of both ions at large internuclear separation

$$E_k^{\mathrm{Coul}}=\frac{q_1q_2}{R_0} . \quad (4)$$

A narrow distribution of kinetic energies is expected around this value because of the initial distribution of internuclear distances in the vibrational ground state, given by $|\psi_{v=0}(R)|^2$. This model is expected to improve as more electrons are removed from the molecule and to be exact once all electrons are removed. In practice it is not necessary to remove the K-shell electrons because $R_K \ll R_0$. Recently, Sampoll *et al.* [16] have studied the kinetic energy released in CO dissociation caused by 2.4-MeV/amu Ar^{14+} and found that the average values of their measured distributions are systematically higher than the predictions of the Coulomb-explosion model. In contrast to their findings Mathur *et al.* [17] have found lower kinetic energies than the ones predicted by this simple model, for collisions of 5.1-MeV/amu F^{8+} with CO.

We have used the time-difference spectra of the different dissociation channels measured with a weak extraction field to study the validity of the Coulomb-explosion model. If all final repulsive states are Coulombic, as assumed in such a model, then the reflection of the ground-state probability density $|\psi_{v=0}(R)|^2$ off the repulsive potential-energy curve will result in a narrow approximately Gaussian distribution of kinetic energies. The peak values and FWHMs of such distributions were determined from the best fit to the measured time-difference spectra [23]. A typical time-difference spectrum is shown in Fig. 3. It can be seen that the time-difference spectra of highly charged CO are well reproduced by a single Gaussian distribution. On the other hand, for low charge states of CO a single Gaussian is not sufficient and an additional distribution centered around a much higher value of kinetic-energy release is needed in order to reproduce the spectra. In order to make a more quantitative comparison between our data and the Coulomb-explosion model, the most probable kinetic-energy release values evaluated from the data are plotted in Fig. 4 as a function of the product of final charge states q_1q_2. The solid line in the figure represents the prediction of the Coulomb-explosion model E_k^{Coul} given by Eq. (3). For the doubly and triply charged CO we have plotted only the centroid of the most likely component (i.e., the peak position of the distribution). The measured most likely values are in reasonable agreement with the predictions of the Coulomb-explosion model. However, interchanging the charges of C^{q_1+} and O^{q_2+} ions ($q_1<q_2$) reduces the peak value of the KER in contradiction with the prediction of the model (see Table I). This can be attributed to the lower binding energy of C^{q+} in comparison with O^{q+}. To further test the model, the FWHM values of the kinetic-energy release distributions evaluated from the data are plotted in Fig. 5 as a function

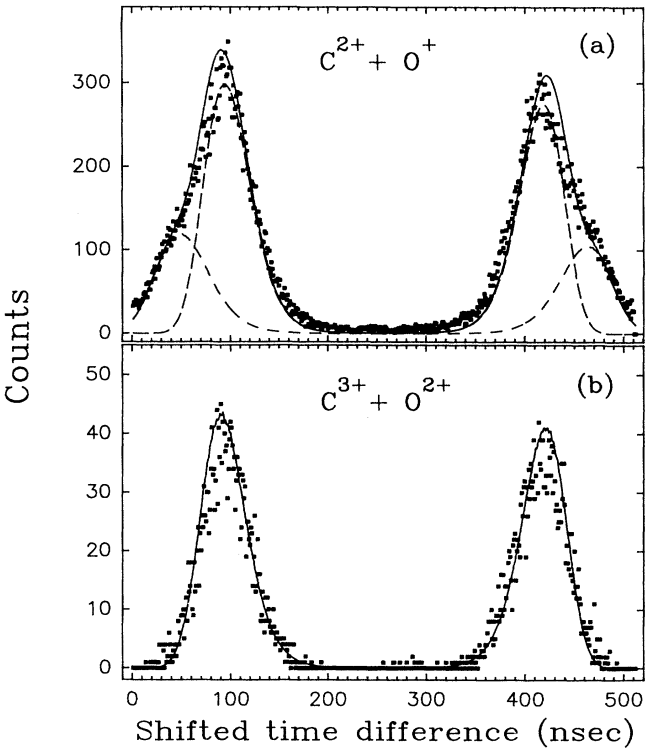

FIG. 3. Measured and simulated time-difference spectra of CO dissociation caused by 1-MeV/amu F^{4+} impact. The simulated spectra was calculated for a Gaussian kinetic-energy release distribution. A weak extraction field of 156 V/cm was used for these measurements. (a) $C^{2+}+O^{+}$, simulated by the sum of two Gaussians centered around 25 and 35 eV, with FWHMs of 9 and 11 eV, respectively. (b) $C^{3+}+O^{2+}$, simulated by a single Gaussian centered around 78 eV with a FWHM of 40 eV.

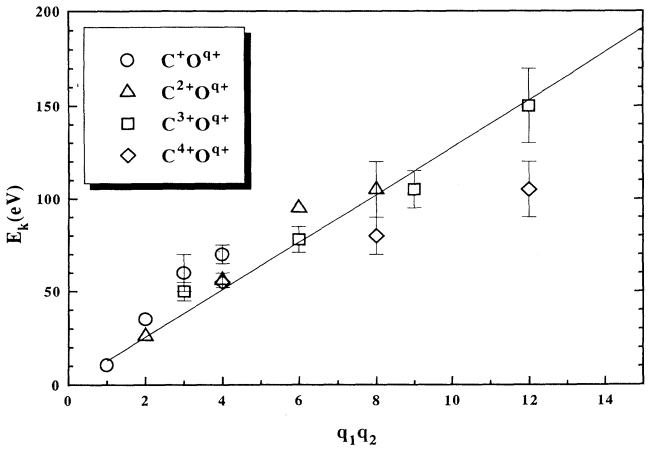

FIG. 4. Most likely values of kinetic-energy release in CO^{Q+} dissociation as a function of q_1q_2. The solid line was calculated using the Coulomb-explosion model.

of the product of final charge states q_1q_2. The measured FWHM increases rapidly from 7±2 eV for C^+ to O^+ to about 50±15 eV for highly charged fragments. Assuming repulsive Coulomb potential-energy curves for the dissociating states, which is the basis of the Coulomb-explosion model, the expected FWHM was calculated by reflecting the vibrational ground-state probability density $|\psi_{v=0}(R)|^2$ off the q_1q_2/R_0 Coulomb potential-energy curve [24]. The calculated FWHM values, indicated by the solid line in Fig. 5, are much smaller than the measured ones. This suggests that the dissociating repulsive states are not all Coulombic. Furthermore, the fact that

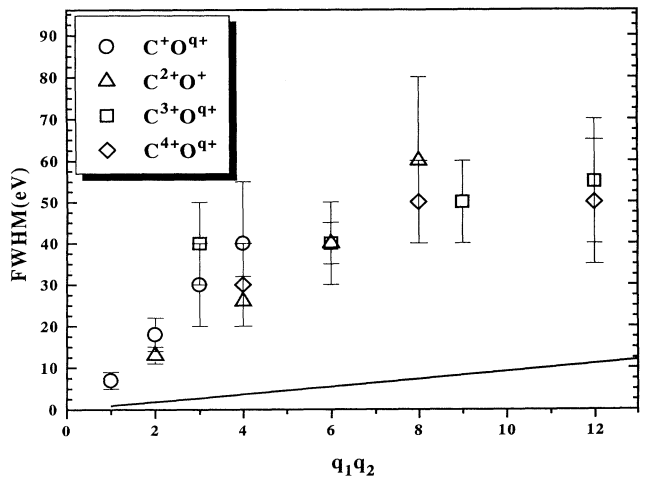

FIG. 5. FWHM values of kinetic-energy release distributions of CO^{Q+} dissociation as a function of q_1q_2. The solid line represents the expected width for dissociation along repulsive Coulomb potential-energy curves, i.e., the Coulomb-explosion model.

the distribution is wider on both the lower- and higher-energy sides of the distribution indicates that both steeper and shallower repulsive potential-energy curves are populated in the collision.

To further study the kinetic-energy release distributions, the time-difference spectra measured with a strong extraction field have been used to evaluate these distributions. This can be done only for the main dissociation channels for which the statistics are good enough. Figure 6 shows the kinetic-energy distribution of the main ion-pair dissociating channels: $C^+ + O^+$, $C^{2+} + O^+$, $C^+ + O^{2+}$, and $C^{2+} + O^{2+}$. It can be seen that, in addition to the most likely peak around the energy predicted by the Coulomb-explosion model, some higher- and even lower-energy contributions are present in some of the dissociation channels. These distributions show trends similar to those reported by Sampoll *et al.* [16]. The fact that we have found the Coulomb-explosion model to agree with the peak position of the distribution while Sampoll *et al.* have found disagreement between the same model and their measured average values is not in contradiction, but an indication that the distributions are not exactly symmetric. They typically have a long high-energy tail; thus the average value is significantly larger than the peak position. The comparison between our data and the higher precision data of Mathur *et al.* [17] cannot be made easily because in their measurement the kinetic energy of a single charged fragment was measured and thus more than one dissociation channel could have been contributing to the measured energy. In our measurements both charged fragments are identified by the coincidence condition, thus selecting a single dissociation channel. Coincidence measurements with similar high precision have been done by Edwards and Wood [24], but not for CO targets. The kinetic-energy distribution of the $C^{2+} + O^{2+}$ dissociation channel is typical for the breakup of highly charged CO molecular ions. This distribution is relatively smooth and its asymmetry is not too large such that it can be approximated by a single Gaussian, as we have done in our treatment of the weak-extraction-field data discussed previously.

There is an interesting trend that can be observed in the kinetic-energy distributions shown in Fig. 6. In most of these distributions, the most prominent peak corresponds to a kinetic-energy release value which is close to the value predicted by the Coulomb-explosion model for that dissociating channel. [This is not the case for the $C^+ + O^{2+}$ breakup, as can be seen from Fig. 6(d)]. The subsequent peaks appear at energy values which are close to the predicted values for the next charge state of the molecular ion. As an example, consider CO^{2+} breaking up into C^+ and O^+. The main peak occurs at 12 eV, which is close to the 12.8-eV value predicted by the Coulomb-explosion model. The next peak in the spectrum occurs roughly at 24 eV, close to the 25.5-eV value predicted by the Coulomb-explosion model for the breakup of CO^{3+} into either $C^+ + O^{2+}$ or $C^{2+} + O^+$. The nice agreement between the predicted and measured second peak position leads to the suggestion that the second peak in the kinetic-energy distribution shown in Fig. 6(a) corresponds to the breakup of a highly excited CO^{2+*}

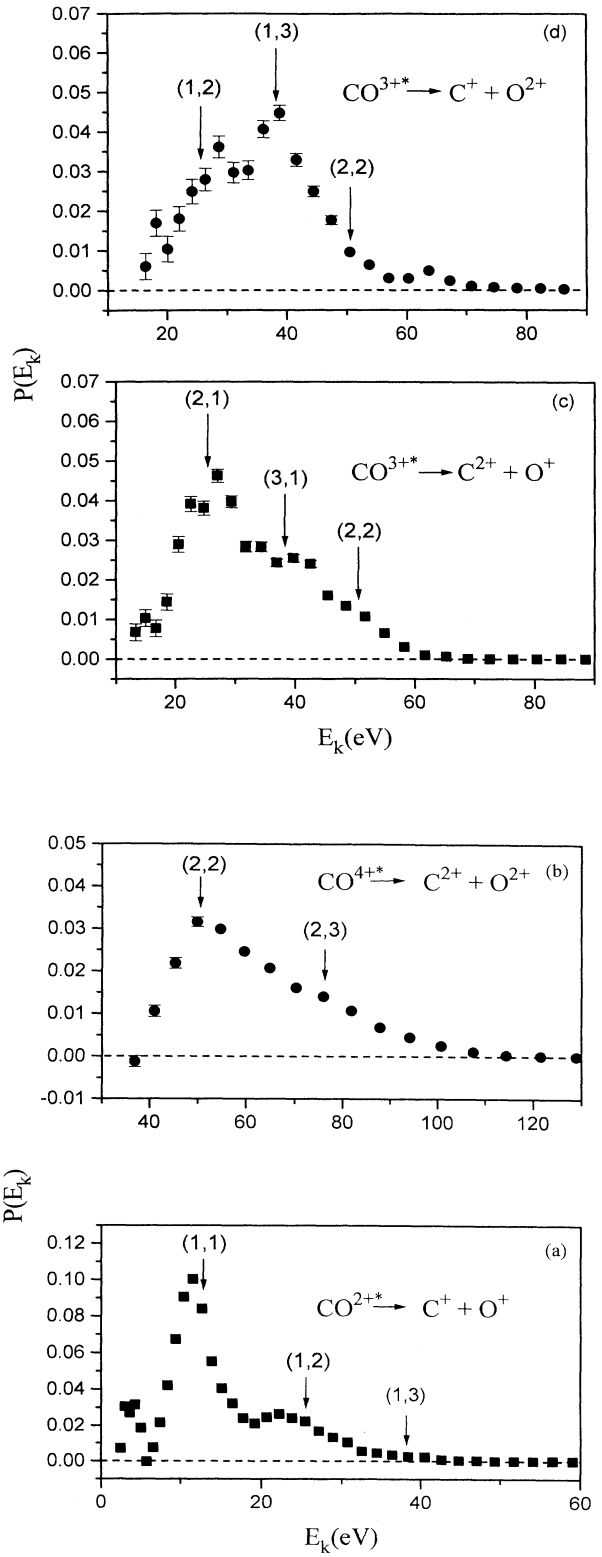

FIG. 6. Kinetic-energy release distributions for the main dissociation channels of CO^{Q+} (Q=2–4): (a) $C^+ + O^+$, (b) $C^{2+} + O^{2+}$, (c) $C^{2+} + O^+$, and (d) $C^+ + O^{2+}$. The arrows mark the kinetic-energy release expected for a (q_1, q_2) breakup within the Coulomb-explosion model.

molecular ion, wherein one valence electron is in a highly excited state so that its contribution to the screening of the nuclear charge is negligible. For such states, the dissociating doubly charged molecular ion behaves like a triply charged molecular ion and therefore releases energy upon breakup which is close to that released during a Coulomb-explosion of a triply charged molecular ion. The kinetic-energy release corresponding to Coulombic breakup of $CO^{Q+} \rightarrow C^{q_1+} + O^{q_2+}$ has been marked as (q_1, q_2) on Fig. 6 for the different breakup channels. Contributions from partly screened states, similar to the ones discussed for $CO^{2+} \rightarrow C^+ + O^+$ breakup, are clearly seen.

The kinetic-energy distribution resulting from the breakup of CO^{2+} into a C^+ and O^+ ion pair following a collision with 1-MeV/amu F^{4+}, shown in Fig. 6(a), has three main kinetic-energy components centered around 4, 12, and 24 eV. This distribution is compared in Fig. 7 to similar distributions measured for 110-eV photons [13], 1-MeV/amu H^+ (will be published elsewhere), and 97-MeV Ar^{14+} [16]. It can be seen from the figure that all the distributions peak approximately at the same value of 12 eV. The kinetic-energy distribution corresponding to the collision between H^+ and CO seems better resolved that that of F^{4+} impact, which in turn has more prominent structure than the one obtained from 97-MeV collisions between Ar^{14+} and CO. In addition, there is definitely more of a contribution from the larger kinetic-energy release values in the case of Ar^{14+} impact. This indicates that an increase in the charge state of the incoming projectile, i.e., an increase in the interaction strength, results in more efficient population of high-lying dissociating states of the molecular ion. In order to make a more quantitative statement, experiments need to be performed in which the velocity of the incoming projectile is kept fixed and its charge q is varied.

The kinetic-energy distribution as obtained from the experiment has also been compared to the distribution calculated using the reflection method. In order to determine the overall kinetic-energy distribution due to the dissociation of CO^{2+*}, it is necessary to determine the individual kinetic-energy distribution associated with each dissociating state of the CO^{2+} molecular ion. This was achieved by reflecting the CO (v=0) wave function off the dissociating CO^{2+} state of interest [25] (see Fig. 8). The potential-energy curves describing the different dissociating states of the CO^{2+} molecular ion, required for the calculation, were taken from Lablanquie *et al.* [13]. The weighted sum of the different kinetic-energy distributions thus obtained were then fit to the measured one as shown in Fig. 9. The calculated distribution for $CO^{2+*} \rightarrow C^+ + O^+$ reproduces the main features of the measured one. A few differences between the calculated and measured kinetic-energy distributions are as follows.

(i) The low-energy peak is not accounted for in the calculated distribution. This is because the low-energy component of the distribution is due to the dissociation of metastable CO^{2+} molecular ions via the tunneling mechanism [26]; these states have not been included in the theoretical fit.

(ii) The high-energy tail of the calculated distribution

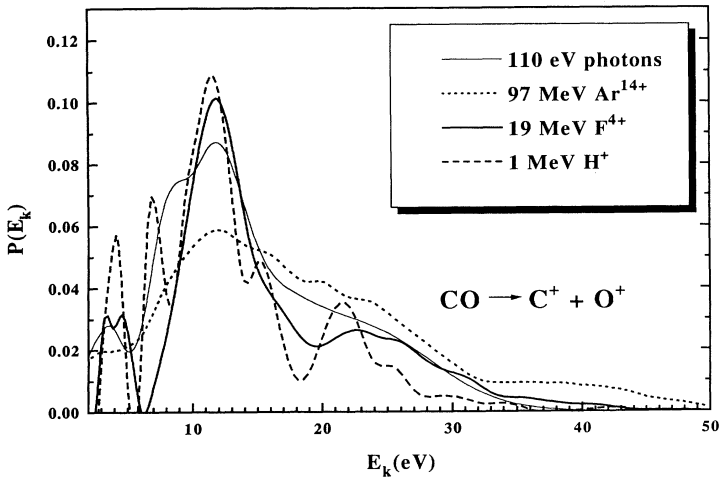

FIG. 7. Kinetic-energy release distributions for the dissociation of CO^{2+} into $C^+ + O^+$. The two electrons were removed from the CO by different fast projectiles: 110-eV photons [13], 97-MeV Ar^{14+} [16], 1-MeV/amu F^{4+} and H^+(will be published elsewhere).

does not extend as far as the experimental one. There are two possible reasons for missing high-kinetic-energy release values in the calculated distribution.

(a) In principle, all the dissociating states should be used in the computation of the kinetic-energy distribution. This, however, was not the case in our calculations, since only some of the low-lying dissociating states of CO^{2+} have been reported. Therefore, the contributions of the highly excited states, which would affect the tail of the distribution, are not accounted for, causing the discrepancy between the measured and calculated distributions.

(b) We have also not included dissociation of one state via another due to "curve crossing." These would also contribute to the high-energy tail of the distribution as shown in Fig. 8.

The weights corresponding to the different final disso-

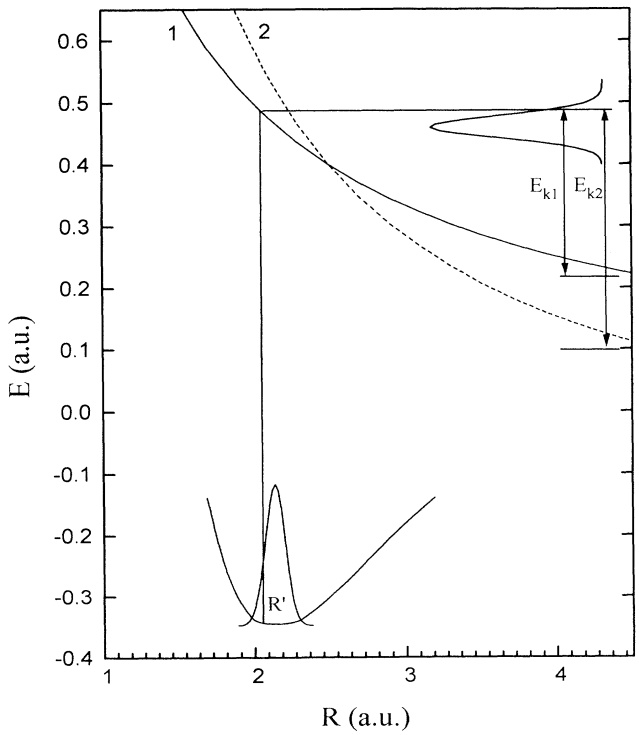

FIG. 8. Schematic representation of the reflection method. The kinetic-energy distribution resulting from the molecule dissociating via a curve crossing is also shown.

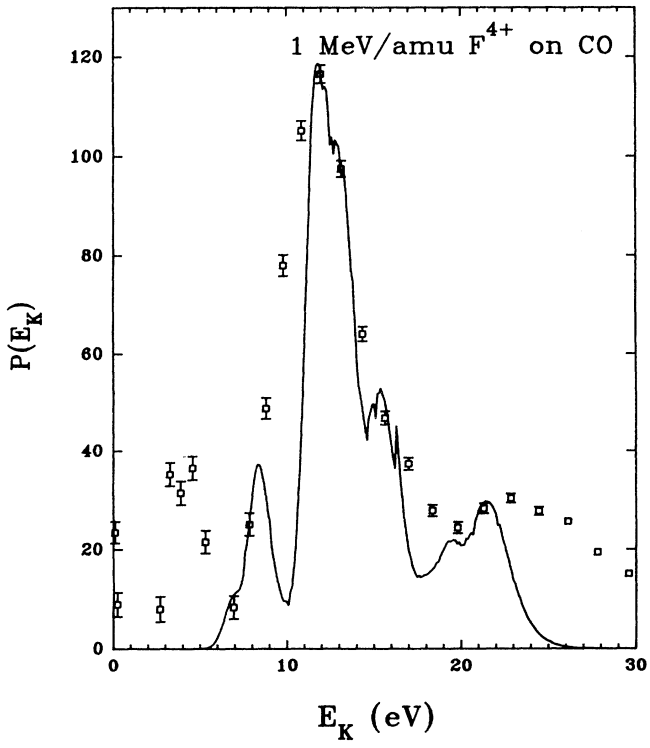

FIG. 9. Kinetic-energy release distribution for the dissociation of CO^{2+} into $C^+ + O^+$ caused by 1-MeV/amu F^{4+}. The solid line is a fit of the sum of all transitions from the CO vibrational ground state to all known repulsive states of CO^{2+} using the reflection method, as explained in the text.

ciating states, which were used as the fitting parameters, correspond to the transition probabilities from the CO ground state to the different dissociating states of CO^{2+}. The motivation behind this exercise was to determine whether there is any propensity rule associated with the different symmetries of the final CO^{2+} states, i.e., is it more likely to populate final molecular states of a specific symmetry. No such rule was found to exist. However, if the transition probability is plotted as a function of the transition energy at R_0, as shown in Fig. 10, an interesting trend can be seen. It appears that there is a "window" in the transition energy (the energy required for the CO to CO^{2+*} transition), between 46 and 58 eV, within which the probability of populating a dissociating state is substantial, whereas the probability falls rapidly on either side of this window. It is unclear as to why such a window should exist. It is our conjecture that this might be caused by the existence of a range of impact parameters b within which double ionization proceeds efficiently. For the fast collisions of interest in our study it is known that single ionization is associated with very soft collisions (i.e., large b), while multiple ionization is associated with hard collisions (i.e., small b) [27]. Thus the exclusive double ionization is limited to intermediate impact parameters because single ionization is dominating it at large impact parameters and triple ionization is taking over at smaller values of b. Using the independent-electron approximation, the probability for double ionization of CO is proportional to

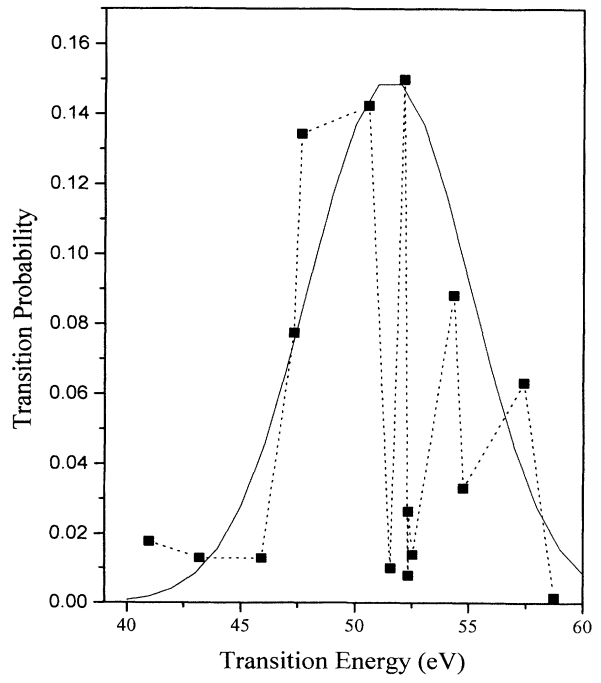

FIG. 10. Transition probability as a function of the transition energy (i.e., the energy required to ionize CO into the corresponding dissociating state of CO^{2+}). The dotted line is drawn to guide the eye and the solid is a Gaussian representing qualitatively the window of transition energies which are more likely to happen.

$$\binom{N}{2} P_i^2(b)[1-P_i(b)]^{N-2}, \tag{5}$$

where $P_i(b)$ is the ionization probability of the active electron and N is the number of equivalent electrons (for CO it is reasonable to assume that all ten valence electrons are equivalent). For highly charged projectiles the ionization probability at small impact parameters is relatively large (because of the q^2 scaling); thus the $[1-P_i(b)]^{N-2}$ term in the double-ionization probability is very small for small b, while for large b the active electron ionization probability falls off rapidly and a window for double ionization is formed. This window in the impact-parameter range for exclusive multiple ionization of Ne has been discussed in detail for collisions of highly charged ions at the same velocity as this work [28]. For example, single ionization of Ne by 1-MeV/amu Ne^{10+} starts around 2 a.u. and is effective over a large range of impact parameters, tailing off at around 10 a.u. Double and triple ionization, however, have a much shorter range, extending between 1.5–6 and 1.2–4.5 a.u., respectively [28]. It has also been shown that at our collision velocities, single and double ionization of Ne and CO are not very different from each other [14]. It is therefore reasonable to expect a similar window of impact parameters. Such a window of impact parameters will result in a window of transition energies because the interaction strength spans a finite range from q/vb_{max} to q/vb_{min} and is strongly peaked around the impact-parameter value where the double-ionization probability given in Eq. (5) has a maximum. This typical behavior of an exclusive multielectron process for a many-electron target could be the explanation for the observed transition energy window. It would be interesting to see how this window is affected by changing the charge or the velocity of the impinging projectile.

IV. CONCLUSIONS

The kinetic energy released during the dissociation of multiply charged CO^{Q+} molecular ions formed in collisions of 1-MeV/amu F^{4+} and CO has been studied using coincidence time-of-flight spectrometry. The measured "most probable" kinetic-energy release values for the different CO^{Q+} molecular ions can be approximately predicted by the Coulomb-explosion model. However, the widths of the kinetic-energy distributions are underestimated by the model. Furthermore, the distributions have both low- and high-energy tails. This suggests that potential-energy curves with steeper and shallower slopes as compared to that of the Coulombic potential-energy curve are populated during the collision.

The kinetic-energy distribution of the $CO^{2+} \rightarrow C^+ + O^+$ breakup channel produced by 1-MeV/amu H^+, 1-MeV/amu F^{4+}, and 97-MeV Ar^{14+} impact shifts to higher values with an increase in the charge of the impinging ion. In spite of this shift the peak of the distribution is approximately fixed and is in agreement with the predicted value of the Coulomb-explosion model. More experiments are needed to study the quantitative dependence of the distributions on the charge state of

the projectile. The measured kinetic-energy distribution of the $C^+ + O^+$ breakup channel caused by 1-MeV/amu F^{4+} impact was fit to the distribution resulting from transitions from the CO ground state to all available CO^{2+} dissociating states. The transition probabilities to the different dissociating states were used as the fitting parameters. No propensity rule was found with respect to the symmetries of the different states of the dissociating CO^{2+} molecular ion. However, there seems to be a window of transition energies, between 46 and 58 eV, which are more preferred than the others. It is unclear as to why there should be such a window, but it could be explained by the window of impact parameters associated with double ionization of a many-electron target by a fast highly charged ion.

ACKNOWLEDGMENTS

We would like to thank Z. Chen for helping us determine the CO $v=0$ wave function. We would also like to thank P. Lablanquie, J. M. Robbe, and G. Gandara for sending us tables of the potential-energy curves of CO^{2+}. This work was supported by the Division of Chemical Sciences, Office of Basic Energy Sciences, Office of Energy Research, U.S. Department of Energy.

[1] K. Boyer, T. S. Luk, J. C. Solem, and C. K. Rhodes, Phys. Rev. A **3**, 1186 (1989).
[2] L. J. Frasinski, K. Codling, and P. A. Hatherly, Science **246**, 10 (1989).
[3] C. Cornaggia, J. Lavancier, D. Normand, J. Morellec, and H. X. Liu, Phys. Rev. A **42**, 5464 (1990).
[4] W. T. Hill, J. Zhu, D. L. Hatten, Y. Cui, J. Goldhar, and S. Yang, Phys. Rev. Lett. **69**, 2646 (1992).
[5] T. J. Gray, J. C. Legg, and V. Needham, Nucl. Instrum. Methods Phys. Res. Sect. B **10/11**, 253 (1985).
[6] R. J. Maurer, C. Can, and R. L. Watson, Nucl. Instrum. Methods Phys. Res. Sect. B **27**, 5 (1987).
[7] H. Tawara, T. Tonuma, H. Kumagai, and T. Matsuo, Phys. Scr. **42**, 434 (1990).
[8] D. Mathur, E. Krishnakumar, F. A. Rajgara, U. T. Raheja, and V. Krishnamurthi, J. Phys. B **25**, 2997 (1992).
[9] I. Ben-Itzhak, S. G. Ginther, and K. D. Carnes, Nucl. Instrum. Methods Phys. Res. Sect. B **66**, 401 (1992).
[10] H. Lebius and B. A. Huber, in *The Physics of Highly Charged Ions*, edited by P. Richard, M. Stöckli, and C. D. Lin, AIP Conf. Proc. No. 274 (American Institute of Physics, New York, 1993), p. 218.
[11] A. P. Hitchcock, P. Lablanquie, P. Morin, E. Lizon, A. Lugrin, M. Simon, P. Thirty, and I. Nenner, Phys. Rev. A **37**, 2448 (1988).
[12] P. Lablanquie, J. Delwiche, M.-J. Franskin-Hubin, I. Nenner, J. H. D. Eland, and K. Ito, J. Mol. Struct. **174**, 41 (1988).
[13] P. Lablanquie, J. Delwiche, M-J. Franskin-Hubin, I. Nenner, P. Morin, K. Ito, J. H. D. Eland, J.-M. Robbe, G. Gandara, J. Fournier, and P. G. Fournier, Phys. Rev. A **40**, 5673 (1989).
[14] I. Ben-Itzhak, S. G. Ginther, and K. D. Carnes, Phys. Rev. A **47**, 2827 (1993).
[15] V. Frohne, S. Cheng, R. Ali, M. Raphaelian, C. L. Cocke, and R. E. Olson, Phys. Rev. Lett. **71**, 696 (1993).
[16] G. Sampoll, R. L. Watson, O. Heber, V. Horvat, K. Wohrer, and M. Chab, Phys. Rev. A **45**, 2903 (1992).
[17] D. Mathur, E. Krishnakumar, K. Nagesha, V. R. Marathe, V. Krishnamurthi, F. A. Rajgara, and U. T. Raheja, J. Phys. B **26**, L141 (1993).
[18] S. L. Varghese, C. L. Cocke, S. Cheng, E. Y. Kamber, and V. Frohne, Nucl. Instrum. Methods Phys. Res. Sect. B **40/41**, 266 (1989).
[19] S. Cheng, C. L. Cocke, V. Frohne, E. Y. Kamber, and S. L. Varghese, Nucl. Instrum. Methods Phys. Res. Sect. B **56/57**, 78 (1991).
[20] R. L. Ezell, A. K. Edwards, R. M. Wood, M. W. Dittmann, J. F. Browning, and M. A. Mangan, Nucl. Instrum. Methods Phys. Res. Sect. B **56/57**, 292 (1991).
[21] K. Schäfer, W. Y. Baek, K. Förster, D. Gassen, and W. Neuwrith, Z. Phys. D **21**, 137 (1991).
[22] I. Ben-Itzhak, S. G. Ginther, and K. D. Carnes, in *The Physics of Highly Charged Ions* (Ref. [10]), p. 343.
[23] S. G. Ginther, Masters thesis, Kansas State University, 1992.
[24] A. K. Edwards and R. M. Wood, J. Chem. Phys. **76**, 2938 (1982).
[25] A. S. Coolidge, H. M. James, and R. D. Present, J. Chem. Phys. **4**, 193 (1935).
[26] V. Krishnamurthi, K. Nagesha, V. R. Marathe, and D. Mathur, Phys. Rev. A **44**, 5460 (1991).
[27] T. J. Gray, C. L. Cocke, and E. Justiniano, Phys. Rev. A **22**, 849 (1980).
[28] I. Ben-Itzhak, T. J. Gray, J. C. Legg, and J. H. McGuire, Phys. Rev. A **37**, 3685 (1988).